NCA-Vol. 26

Proceedings of the ASME

NOISE CONTROL AND ACOUSTICS DIVISION — 1999

- INNOVATIVE EXPERIMENTAL AND NUMERICAL TECHNIQUES IN STRUCTURAL VIBRATION AND ACOUSTICS
- TURBOMACHINERY NOISE
- AUTOMOTIVE NOISE AND VIBRATION
- BS/MS STUDENT PAPER COMPETITION
- MULTIFUNCTIONAL MATERIALS AND STRUCTURES
- ACOUSTIC SENSING, IMAGING, AND INVERSE PROBLEMS
- FLOW-INDUCED VIBRATION AND NOISE OF THIN MATERIALS
- COMPUTATIONAL ACOUSTICS

presented at
THE 1999 ASME INTERNATIONAL MECHANICAL ENGINEERING CONGRESS AND EXPOSITION
NOVEMBER 14–19, 1999
NASHVILLE, TENNESSEE

sponsored by
THE NOISE CONTROL AND ACOUSTICS DIVISION, ASME

principal editor
SEAN F. WU
WAYNE STATE UNIVERSITY

contributing editors

NICKOLAS VLAHOPOULOS
UNIVERSITY OF MICHIGAN

MARDI C. HASTINGS
OHIO STATE UNIVERSITY

MARTIN L. POLLACK
LOCKHEED MARTIN

YUN-FAN HWANG
PENN STATE UNIVERSITY

EMMANUEL O. AYORINDE
WAYNE STATE UNIVERSITY

RICHARD C. MARBOE
PENN STATE UNIVERSITY

JEFFREY CIPOLLA
H. K. S. INC.

MARTIN DUNN
UNIVERSITY OF COLORADO

THEODORE M. FARABEE
NAVAL SURFACE WARFARE CTR.

NIRANJAN HUMBAD
VISTEON, FORD

PAUL E. BARBONE
BOSTON UNIVERSITY

RAYMOND J. NAGEM
BOSTON UNIVERSITY

KARL GROSH
UNIVERSITY OF MICHIGAN

YOUNG BAE CHANG
OKLAHOMA STATE UNIVERSITY

ALLAN D. PIERCE
BOSTON UNIVERSITY

THE AMERICAN SOCIETY OF MECHANICAL ENGINEERS
Three Park Avenue / New York, N.Y. 10016

Statement from By-Laws: The Society shall not be responsible for statements or opinions advanced in papers. . . or printed in its publications (7.1.3)

INFORMATION CONTAINED IN THIS WORK HAS BEEN OBTAINED BY THE AMERICAN SOCIETY OF MECHANICAL ENGINEERS FROM SOURCES BELIEVED TO BE RELIABLE. HOWEVER, NEITHER ASME NOR ITS AUTHORS OR EDITORS GUARANTEE THE ACCURACY OR COMPLETENESS OF ANY INFORMATION PUBLISHED IN THIS WORK. NEITHER ASME NOR ITS AUTHORS AND EDITORS SHALL BE RESPONSIBLE FOR ANY ERRORS, OMISSIONS, OR DAMAGES ARISING OUT OF THE USE OF THIS INFORMATION. THE WORK IS PUBLISHED WITH THE UNDERSTANDING THAT ASME AND ITS AUTHORS AND EDITORS ARE SUPPLYING INFORMATION BUT ARE NOT ATTEMPTING TO RENDER ENGINEERING OR OTHER PROFESSIONAL SERVICES. IF SUCH ENGINEERING OR PROFESSIONAL SERVICES ARE REQUIRED, THE ASSISTANCE OF AN APPROPRIATE PROFESSIONAL SHOULD BE SOUGHT.

ISBN No. 0-7918-1637-0

ISSN No. 1522-1415

NCA-Vol. 26, Proceedings of the ASME
Noise Control and Acoustics Division — 1999
ASME 1999

BASIC ANALYTICAL MODELING OF THE PISTON SLAP IN CONJUNCTION WITH ENGINE BLOCK VIBRATION

Saeed J. Siavoshani, Ph.D.,
Powertrain Division
General Motors Corporation
Warren, Michigan

Michael A. Latcha, Ph.D.,
Dept of Mechanical Engineering
Oakland University
Rochester, Michigan

ABSTRACT

The objective of this research is to enhance and develop analytical and experimental schemes to study the source and path analysis of piston slap noise and to develop tools to relate the piston slap to the engine block vibration. These computer tools solve the piston dynamics and the engine block vibration. The results of this approach are block vibrations that are comparable to experimental results. This study resulted in an analytical approach to understand the piston dynamics in conjunction with block vibration. The engine block vibration was obtained using both a coupled and uncoupled approach due to the piston slap. The coupled approach was to solve the piston motion along with the flexible motion of the cylinder bore which yields the cylinder block vibration directly. The uncoupled approach consists of solving for the contact forces with the simple cylinder model; then using those forces in an FEA analysis of the engine block to determine the resulting vibration.

I. INTRODUCTION

Piston slap is now recognized as one of the major sources of noise pollution in automotive engines, both diesel and gasoline. Recently, it has also been a major issue with manufacturer warranties, as unhappy customers have been returning automobiles because of noise. Although governmental regulations played a part in the partial reduction of noise pollution, it was customer demand that put the subject of noise and vibration on an equal footing with other engineering directives and challenges. Since the invention of the automobile, piston noise has simply been one of those drawbacks that comes from advancing technology. In the earlier years of the automobile, noise wasn't considered an important aspect of a better engine design. As more autos came into use, the noise problem became more significant--especially in diesel engines, which made up a better part of the noise problem. Moreover, as gasoline engines became faster and more powerful, the noise increased. The 1960's saw the first attempt at governmental noise regulations that directed its efforts toward the automotive industry.[1]

As global competition entered the scene in the 1970's, the automotive industry was forced to push for not only faster, more powerful engines, but quieter ones as well. Customer satisfaction soon became the goal for an increase in noise and vibration research and development. In the late 1970's, research was done to design better tools to analyze piston slap rather than rely on the traditional "human ear."[2] Working toward this alternative approach, research showed that by analyzing the dynamics of piston movement within the bore, piston slap was discovered to be one of the origins of mechanical vibrations within the engine itself. Reducing the clearance between the piston and the bore was thought to be the best way to reduce piston slap noise. Unfortunately, it also resulted in decreased mechanical efficiency because the piston forces caused too much friction and vibration, resulting in both scuffing and wear of the piston and engine. In the late 1970's, an alternative method was developed by DeJong[3] to study piston slap noise and vibration without reducing the clearance between the piston and the cylinder bore liner. In his work, DeJong emphasized a better understanding of the transmission path of the piston slap noise and block vibration. It was hoped that his alternative liner combined with a future piston-bore clearance would even further reduce the piston slap and cylinder bore noise and vibration.

In the early 1980's, the Society of Automotive Engineers sponsored an engine noise conference involving the developments in engine noise research, piston movement and piston influence upon automotive engines. Experts concerned with noise and vibration gathered to accentuate the problems and discuss possible solutions.[4]

Up until 1987, all of the analytical and experimental work toward solving piston slap was mainly focused on piston motion. It should be noted that until that time, little was known concerning the coupling between piston slap and block vibration. In 1987, research provided a solution, which linked the piston motion to the block vibration. This theory presented an analytical model of piston slap, taking into account the equation of motion for the coupled system of piston and cylinder bore vibration.[5]

Later, in 1995, Kamp and Spermann [6] presented some research of understanding, evaluating and improving piston-related noise in internal combustion engines. He also incorporated the sound quality study of piston slap and cylinder bore vibration using the subjective noise rating scale method. Their piston slap noise work was focused mainly on experimental accomplishments rather than developing analytical models.

Finally, in 1997, Nakada, Yamamoto and Abe[7] from Isuzu presented a numerical approach to study the piston secondary motion and its application. The hydrodynamic behavior and effects of the oil film and friction forces were included. They also emphasized the use of kinetic energy of the piston skirt with block vibration measurements and the relationships between them.

By definition, piston slap is caused by the piston as it strikes the major thrust and minor anti-thrust sides in its transverse or secondary motion. Therefore, it is essential to develop a model to understand the piston dynamics in conjunction with the engine block. The piston dynamics include the transverse motion of the piston, the tilting of the piston and the contact forces between the piston and the cylinder bore. The motion of the engine block includes the vibration of the cylinder bore due to the piston slap impact forces. To understand the physics of piston slap, several different computer models were developed and will be discussed in the following sections.

Section 2 explains a simple model of the piston slap that uses a point mass to represent the piston and springs to represent the local stiffness of the cylinder bore. The gap between the point mass and the springs represents the clearance between the piston and the cylinder bore. This model only simulates the secondary motion of the piston as it travels from the major thrust to the minor anti-thrust side.

In Section 3, a more complex model will be discussed, including the cylinder bore vibration using a bar analogy.

Later, in Section 4, a more complicated program will be described which includes the primary and secondary motion of the piston in conjunction with the cylinder bore vibration--the main focus of this study.

Section 5 discusses the engine block vibration due to piston slap. The piston slap impact forces obtained from Section 4 were mapped on the engine block along the major thrust and minor anti-thrust sides of the cylinder bore. The engine block vibration due to the impact forces was obtained.

The entire effort of piston modeling throughout this research has been focused on a single point mass model. The reasons and justifications for this simplification is that the first natural frequency of the typical piston occurs about 3500 Hz, higher than the frequency of interest concerning piston slap. This paper will also model the oil film between the piston and the cylinder bore by using a simple viscous element representation.

2. MASS, SPRING AND VISCOUS OIL FILM WITH RIGID & COMPLIANT CYLINDER BORE

The mathematical model of the piston and cylinder bore is represented using a point mass and spring analogy, in which the springs simulate the local stiffness of the cylinder bore. It should be noted that if a higher spring stiffness is chosen, it represents a more rigid cylinder bore. Simple dampers represent the local oil film between the piston and the cylinder bore and its damping effect. A schematic of the model is given in Figure 1. This model only simulates the transverse or secondary motion of the piston, leading to the impact between the point mass and each side of the cylinder bore represented by the springs. The applied forces on the point mass are caused by the cylinder pressure, the friction forces between the piston and cylinder bore, the friction forces between the piston rings and cylinder bore, the inertia forces and the impact forces. The governing equations describing the point mass traveling from the minor anti-thrust to the major thrust side are as follows:

As the point mass is approaching the minor anti-thrust side, if $x < e$ or $x > -e$, then

$$m\ddot{x} = F_{applied} \qquad (2\text{-}1)$$

describes the equation of motion in the transverse direction. On the other hand, if the point mass has contacted the minor anti-thrust or major thrust sides, if $x > e$ or $x < -e$, then the equation,

$$m\ddot{x} + c_{oil}\dot{x} + K_t(x \mp e) = F_{applied} \qquad (2\text{-}2)$$

governs its dynamic behavior. C_{oil} represents the oil between the piston and the cylinder bore while e represents the clearance between the two. These two equations can be re-written in the matrix form:

$$[M]\ddot{x} + [C]\dot{x} + [K]x = F_{applied} \qquad (2\text{-}3)$$

Using state space variables, the new variables are defined as follows:

$$x = y_1 \qquad \dot{x} = \dot{y}_1 = y_2 \qquad (2\text{-}4)$$

By placing Equation 2-4 into Equation 2-3, the following equations can be obtained:

$$\dot{y}_1 = y_2 \qquad (2\text{-}5)$$

$$\dot{y}_2 = -\frac{K_t}{m}y_1 - \frac{c_{oil}}{m}y_2 \pm \frac{K_t}{m} + F_{applied}$$

(2-6)

These two equations can be rearranged into a final matrix form, which follows:

$$\begin{bmatrix}\dot{y}_1\\ \dot{y}_2\end{bmatrix} = \begin{bmatrix}0 & 1\\ -\frac{K_t}{m} & -\frac{c_{oil}}{m}\end{bmatrix}\begin{bmatrix}y_1\\ y_2\end{bmatrix} + \begin{bmatrix}0\\ \pm\frac{K_t}{m} + F_{applied}\end{bmatrix} \qquad (2\text{-}7)$$

These equations were solved using MATLAB ODE23S [8] based on a modified Rosenbrock formula of order 2, with a time interval of 10^{-6} seconds. The output of the program includes impact forces, point mass transverse displacement and velocity of the impact.

Figure 2 shows the piston transverse motion as a function of time. As Figure 2 indicates, when the point mass strikes the cylinder bore, it penetrates inside, to a point where the forces are balanced. The direction of the force changes as the point mass rebounds against the bore and moves toward the other side.

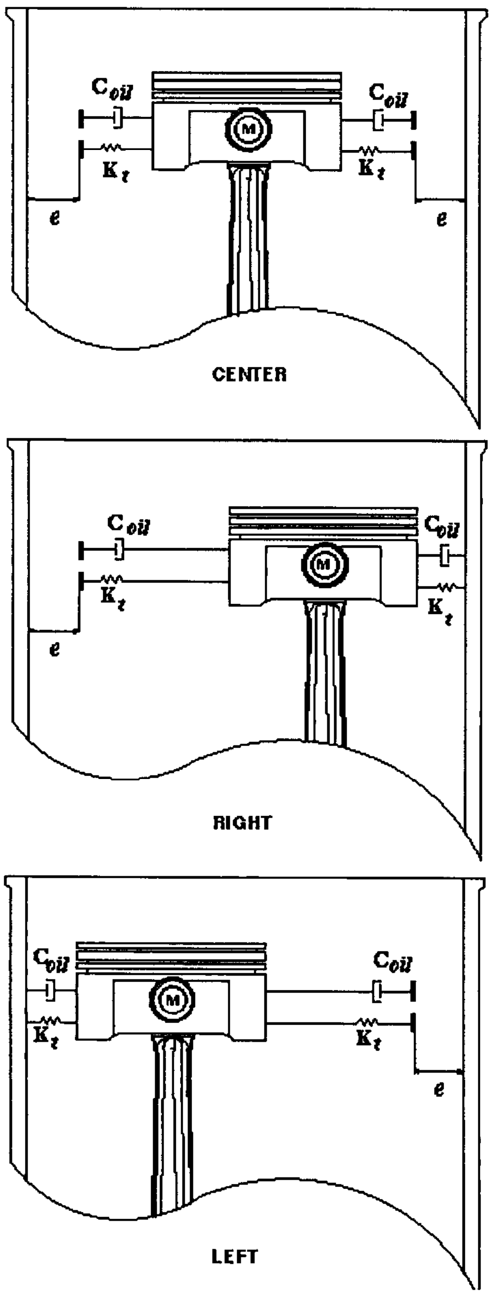

Figure 1: Schematic of Mathematical Model of Piston and Cylinder Bore Represented by a Point Mass and Spring Analogy where the left side of the cylinder bore is called the major side and the right side is the minor side.

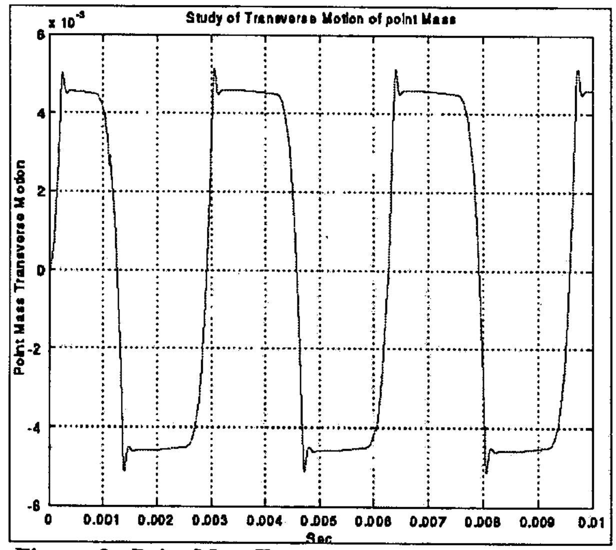

Figure -2: Point Mass Transverse Motion

3. MASS, SPRING AND VISCOUS OIL FILM WITH CYLINDER BORE VIBRATION

To extend the capability of the model, the next analytical step was to include the cylinder bore vibration. In Section 2, the mathematical models of the piston and bore were represented using a point mass and spring analogy, respectively. In this section, the point mass continues to represent the piston, but the cylinder bore is represented by a bar analogy to model the cylinder bore vibration. A schematic of the model is given is Figure 3.

This figure represents three different positions of the point mass with respect to the cylinder bore. The main differential equation describing the transverse motion of the point mass follows:

$$m\ddot{x}_p = F_{applied} + \sum_1^2 F_s \qquad (3\text{-}1)$$

where the applied forces are the same as in Section 2 and the result of the impact forces are represented by $\sum_1^2 F_s$.

The cylinder bore vibration can be described by a summation of independent differential equations that can be represented by a longitudinal bar vibration. The equation of a free vibration of a bar, which is clamped at one end and free at the other end, is given by

$$EA\frac{\partial^2 u}{\partial x^2} = \rho A\frac{\partial^2 u}{\partial t^2} \qquad u(0,t) = 0 \qquad (3\text{-}2)$$

This equation can be solved by the method of separation of variables. The characteristic equation of a bar from which the natural frequencies and mode shapes can be derived as the following[9]:

$$\omega_n = \frac{(2n-1)\pi x}{2l} \quad \Phi\,(x) = B\sin\frac{(2n-1)\pi x}{2l} \quad \text{for } n = 1,2.... \qquad (3\text{-}3)$$

where $\omega_n = \dfrac{(2n-1)\pi x}{2l}$

represents the natural frequency and

$$\Phi(x) = B\sin\frac{(2n-1)\pi x}{2l}$$

provides the mode shapes of the bar. The corresponding eigenfunctions can be normalized with respect to the mass using the modal orthogonality.

$$\int_0^l B^2 \sin\frac{(2n-1)\pi x}{2l}\sin\frac{(2m-1)\pi x}{2l}dx = \delta_{nm} = \begin{cases}1 & n=m\\ 0 & n\neq m\end{cases} \quad (3\text{-}4)$$

After integration and simplification, the normalized eigenfunction with respect to the mass of the bar is:

$$\Phi_{normalized}(x) = \sqrt{\frac{2}{ml}}\sin\frac{(2n-1)\pi x}{2l} \quad n=1,2 \quad (3\text{-}5)$$

By placing $x=l$ and $n=1,2$, the normalized eigenvectors corresponding to the free-end tip of the bar can be obtained. For simplicity, only the first two natural frequencies and their corresponding mode shapes were chosen to describe the longitudinal motion of the bar, which are identical for both sides.

$$\Phi_{1,2} = \left[+\sqrt{\frac{2}{ml}} \quad -\sqrt{\frac{2}{ml}}\right] \quad (3\text{-}6)$$

As previously mentioned, the vibration of the bar on both major and minor sides can be represented as a summation of a series of independent differential equations. The following expression represents the longitudinal bar vibration that has been normalized with respect to its mass

$\ddot{\eta}_i(t) + 2\omega_i\eta_i(t)_1 + \omega_i^2\eta_i(t) = f_i$ where

$$f_i = \begin{bmatrix}+\sqrt{\frac{2}{ml}}\\ -\sqrt{\frac{2}{ml}}\end{bmatrix}\sum_1^2 F_s \quad i=1,2 \quad (3\text{-}7)$$

where $\left(\sum_1^2 F_s\right) = \left[F_{mj} \quad F_{mn}\right]$ is the contact force vector that occurs when the point mass strikes the bar in both the major and minor anti-thrust sides and is modeled by a resilient spring and damping element, shown in Figure 3.

The mathematical expression for the force derived at a point of contact, as well as the condition of the point mass striking the bar for both the major thrust and minor anti-thrust sides is expressed as the following conditions:

For the major thrust side	For the minor side:
if $(x_p - x_{bar}) < -e$	*if* $(x_p - x_{bar}) > +e$
$F_{mj1} = -k_p((x_p - (-e)) - x_{bar})$	$F_{mn1} = -k_p((x_p + e) - x_{bar})$
if $(\dot{x}_p - \dot{x}_{bar}) < 0$	*if* $(\dot{x}_p - \dot{x}_{bar}) > 0$
$F_{mj2} = -c_{oil}(\dot{x}_p - \dot{x}_{bar})$	$F_{mn2} = -c_{oil}(\dot{x}_p - \dot{x}_{bar})$
else	*else*
$F_{mj2} = 0.0$	$F_{mn2} = 0.0$
end	*end*
$F_{mj} = F_{mj1} + F_{mj2}$	$F_{mn} = F_{mn1} + F_{mn2}$
else	*else*
$F_{mj} = 0.0$	$F_{mn} = 0.0$
end	*end*

It should be mentioned that for every instant of time, one must check whether there is an impact or not between the piston and the cylinder bore. The above conditions for the major thrust or minor anti-thrust sides must be satisfied. To do this, the generalized coordinates representing the bar should be translated to the physical coordinates. This translation takes place using the following matrix transformation:

$$x_{bar} = \left[+\sqrt{\frac{2}{ml}} \quad -\sqrt{\frac{2}{ml}}\right]\begin{bmatrix}\eta_1\\ \eta_2\end{bmatrix} \quad (3\text{-}8)$$

where η_1 & η_2 are the generalized coordinates representing the bar vibration and $\left[+\sqrt{\frac{2}{ml}} \quad -\sqrt{\frac{2}{ml}}\right]$ is the eigenvector corresponding to the first and the second modes of the bar. To solve the dynamic equations of the point mass and the bar vibration, a series of new variables were defined and substituted into the above equations. Using the state space variable technique, the second degree of freedom equations were transformed to the first degree of freedom equations. The major equations of both the point mass dynamics and the bar longitudinal vibration can be combined and shown as the following:

$$\begin{aligned}
\dot{x}_p &= \dot{y}_1 = y_2\\
\ddot{x}_p &= \dot{y}_2 = \frac{1.0}{m_p}\left(F_{applied} + \sum_1^2 F_s\right)\\
\dot{\eta}_3 &= \dot{y}_7 = y_8\\
\ddot{\eta}_3 &= \dot{y}_8 = -\omega_3 y_7 - 2\xi_3 y_8 + \left(+\sqrt{\frac{2}{ml}}\sum_1^2 F_s\right)\\
\dot{\eta}_4 &= \dot{y}_9 = y_{10}\\
\ddot{\eta}_4 &= \dot{y}_{10} = -\omega_4 y_9 - 2\xi_4 y_{10} + \left(-\sqrt{\frac{2}{ml}}\sum_1^2 F_s\right)
\end{aligned} \quad (3\text{-}9)$$

Of these equations, the first two describe the transverse motion of the point mass and the latter equations represent the first two modes of the longitudinal bar vibration for both major thrust and minor anti-thrust sides. MATLAB was used to solve the non-linear equations and obtain the transverse motion of the point mass, the contact forces and the vibration of the bar. Here, the Runge-Kutta method was used to solve the set of differential equations. The results of the transverse motion of the point mass and bar vibration as functions of time are given in Figures 4 & 5.

As shown in Figure 4, the point mass starts its motion from the center between the right and left bar. It moves toward the positive direction, hitting the bar on one side. It rebounds and travels toward the negative direction, hitting the bar on the other side. The oscillatory motion of the point mass repeats itself several times. Each time the point mass hits the bar, it pushes it inside while maintaining its own particular motion. As the point mass separates from the bar, the bar oscillates and continues to do so until the point mass returns and strikes the bar again. Figure 5 shows the bar vibration.

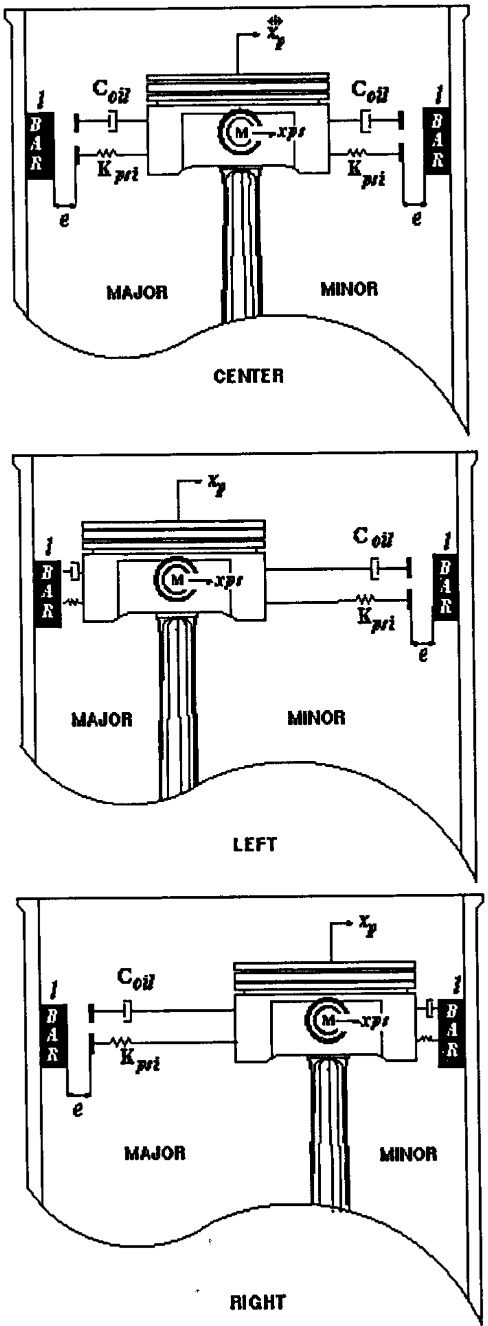

Figure 3: Mass, Spring and Viscous Oil Film with Cylinder Bore Vibration

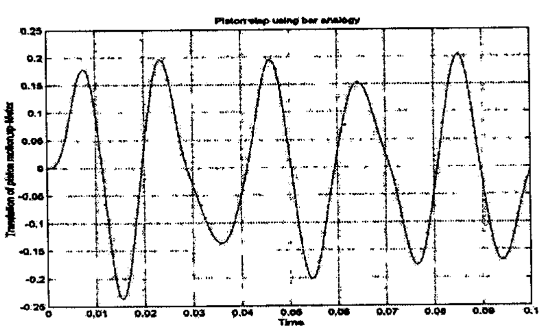

Figure 4: Point Mass Transverse Motion

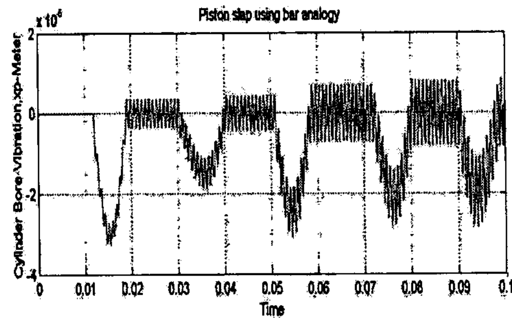

Figure 5: Cylinder Bore Vibration

4. PISTON AND CYLINDER BLOCK SOLUTION TECHNIQUE

The major equations of the piston dynamics were simplified and expressed as the following equations:[10]

$$(m_p + m_r)\ddot{x}_p + m_p\left(L_Y - L_x \tan(\beta)\right)\ddot{\Theta}_p = f_x \qquad (4\text{-}1)$$

$$(I_g + m_p(L_x^2 + L_Y^2))\ddot{\Theta}_p + m_p L_Y \ddot{x}_p = f_\Theta \qquad (4\text{-}2)$$

Equations 4-1 and 4-2 describe the dynamics of the piston independent of the motion of the block. L_x and L_y represent the distance of the piston pin offset with respect to the piston's center of gravity. β is the angle of the connecting rod with respect to the vertical axis. x_p represents the secondary motion and Θ_p represents the tilting degree of freedom of the piston. If the cylinder bore can be represented only by stiffness, then Equations 4-1 and 4-2 are sufficient to obtain the transverse motion of the piston, piston tilt and contact forces. By writing Equations 4-1 and 4-2 into a matrix form, then the resulting transformation is Equation 4-3. The matrix is then inverted to obtain the transverse motion and the tilt of the piston. It should be noted that the inverted matrix is given symbolically here as $\begin{bmatrix} a_{11} & a_{12} \\ a_{21} & a_{22} \end{bmatrix}$ and the details of the matrix elements are left for numerical computation.

$$\begin{bmatrix} m_p + m_r & m_p\left(L_y - L_x \tan(\beta)\right) \\ m_p + L_y & I_g + m_p\left(L_x^2 + L^2{}_y\right) \end{bmatrix} \begin{bmatrix} \ddot{x}_p \\ \ddot{\Theta}_p \end{bmatrix} = \begin{bmatrix} f_x \\ f_\Theta \end{bmatrix} \qquad (4\text{-}3)$$

The solution to the sets of Equations (4-3) provides the piston transverse motion and tilt as well as the impact forces. As mentioned, this solution only includes the stiffness of the cylinder bore. However, if the cylinder bore is represented by stiffness along with inertia, then extra equations describing the cylinder bore vibrations should be added to these sets of equations.

The motion of the cylinder bore can be written as a series of independent single degrees of freedom where each degree of freedom corresponds to an eigenvalue of the cylinder bore. Therefore, the number of equations describing the cylinder bore vibration depends on the number of eigenvalues selected in the solution. The eigenvalues and eigenvectors obtained from the cylinder bore corresponding to the major thrust and minor anti-thrust sides must be normalized with respect to the mass of the model. The normalization of the eigenvectors can be obtained from NASTRAN[11] using the Normal Modes Analysis Solution. In the models developed in this study, the first four eigenvalues and eigenvectors of the cylinder bore were considered which limit the cylinder bore frequency vibration up to 2000 Hz. If higher frequency vibrations of the cylinder bore are desired, then more eigenvalues and corresponding eigenvectors should be included. The modal damping in the following equations have been substituted by the experimental modal damping obtained from the measurements. There, during the course of the eigenvalue extraction of the cylinder bore, using the curve-fitting technique in LMS,[12] the modal damping corresponding to each mode was obtained. The following equations describe the motion of the cylinder bore:

$$\dot{\eta}_1 = \dot{y}_3 = y_4$$

$$\ddot{\eta}_1 = \dot{y}_4 = -\omega^2{}_1 y_3 - 2\xi_1\omega_1 y_4 + \begin{bmatrix} \Phi_{11} & \Phi_{12} & \Phi_{13} & \Phi_{14} \\ \Phi_{21} & \Phi_{22} & \Phi_{23} & \Phi_{24} \\ \Phi_{31} & \Phi_{32} & \Phi_{33} & \Phi_{34} \\ \Phi_{41} & \Phi_{42} & \Phi_{43} & \Phi_{44} \end{bmatrix}^T \left[(-1)\begin{bmatrix} F_{ut} \\ F_{lt} \\ F_{lnt} \\ F_{unt} \end{bmatrix}\right]$$

$$\dot{\eta}_2 = \dot{y}_5 = y_6$$

$$\ddot{\eta}_2 = \dot{y}_6 = -\omega^2{}_2 y_5 - 2\xi_2\omega_2 y_6 + \begin{bmatrix} \Phi_{11} & \Phi_{12} & \Phi_{13} & \Phi_{14} \\ \Phi_{21} & \Phi_{22} & \Phi_{23} & \Phi_{24} \\ \Phi_{31} & \Phi_{32} & \Phi_{33} & \Phi_{34} \\ \Phi_{41} & \Phi_{42} & \Phi_{43} & \Phi_{44} \end{bmatrix}^T \left[(-1)\begin{bmatrix} F_{ut} \\ F_{lt} \\ F_{lnt} \\ F_{unt} \end{bmatrix}\right]$$

$$\dot{\eta}_3 = \dot{y}_7 = y_8$$

$$\ddot{\eta}_3 = \dot{y}_8 = -\omega^2{}_3 y_7 - 2\xi_3\omega_3 y_8 + \begin{bmatrix} \Phi_{11} & \Phi_{12} & \Phi_{13} & \Phi_{14} \\ \Phi_{21} & \Phi_{22} & \Phi_{23} & \Phi_{24} \\ \Phi_{31} & \Phi_{32} & \Phi_{33} & \Phi_{34} \\ \Phi_{41} & \Phi_{42} & \Phi_{43} & \Phi_{44} \end{bmatrix}^T \left[(-1)\begin{bmatrix} F_{ut} \\ F_{lt} \\ F_{lnt} \\ F_{unt} \end{bmatrix}\right]$$

$$\dot{\eta}_4 = \dot{y}_9 = y_{10}$$

$$\ddot{\eta}_4 = \dot{y}_{10} = -\omega^2{}_4 y_9 - 2\xi_4\omega_4 y_{10} + \begin{bmatrix} \Phi_{11} & \Phi_{12} & \Phi_{13} & \Phi_{14} \\ \Phi_{21} & \Phi_{22} & \Phi_{23} & \Phi_{24} \\ \Phi_{31} & \Phi_{32} & \Phi_{33} & \Phi_{34} \\ \Phi_{41} & \Phi_{42} & \Phi_{43} & \Phi_{44} \end{bmatrix}^T \left[(-1)\begin{bmatrix} F_{ut} \\ F_{lt} \\ F_{lnt} \\ F_{unt} \end{bmatrix}\right]$$

Where $\begin{bmatrix} \Phi_{11} & \Phi_{12} & \Phi_{13} & \Phi_{14} \\ \Phi_{21} & \Phi_{22} & \Phi_{23} & \Phi_{24} \\ \Phi_{31} & \Phi_{32} & \Phi_{33} & \Phi_{34} \\ \Phi_{41} & \Phi_{42} & \Phi_{43} & \Phi_{44} \end{bmatrix}$ are the eigenvectors of the points of contact between the piston and the cylinder bore.

By combining the piston equations shown in the sets in 4-1 with the cylinder bore equations, the equations of piston slap in conjunction with the block vibration are obtained. For every instant during the piston primary and secondary motion, the cylinder bore displacement is required. Since the eigenvector information was only available for a limited amount of points on the major thrust and minor anti-thrust sides, a curve-fitting technique was used in both of the analytical and experimental approaches. The eigenvectors obtained were curve-fit using the MATLAB spline function. The curve-fitting information has been implemented in the solution method. The cylinder bore information can then be used to check whether or not there is contact between the piston and the cylinder bore.

These equations were solved using MATLAB. The MATLAB ODE solver functions implement the stiff Runga-Kutta method[13] that requires initial boundary and time conditions. It steps through the time interval, which in this case is 10^{-9} seconds. At every time step, a solution is computed and is checked for solver's error tolerance criteria. Since the problem was concerned with modeling a stiff problem, stiff solvers were used to facilitate the solution procedure. The results obtained from the computer program include piston primary and secondary motion, piston tilt, contact forces between the piston and cylinder bore and the cylinder bore vibration. A few of the results pertaining to the transverse motion of the piston and cylinder bore vibration are given in Figure 6. By observing the transverse motion provided in the figure 6, the piston travels from the bottom dead center to the top while tilting clockwise close to the top dead center. Approximately 15° after the top dead center, when combustion is at peak pressure, the piston has a counter clockwise tilt as well as a translational motion. This complicated motion is a combination of both tilting and rebounding from the minor to the major thrust side.

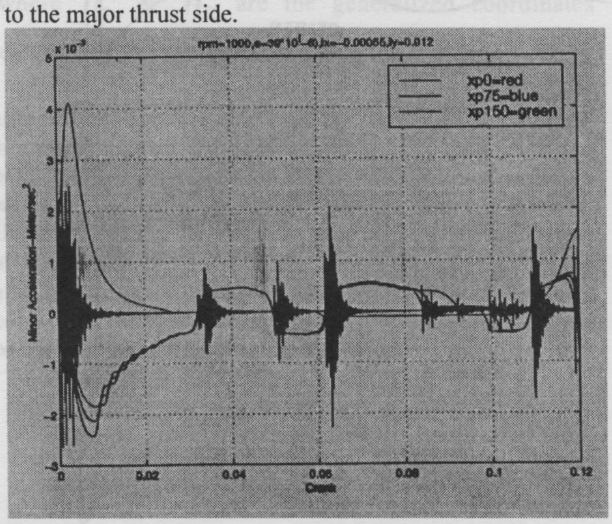

Figure 6: Piston Transverse Motion and Cylinder Bore Vibration

This impact is called piston slap. Later, in the compression cycle, as the piston rebounds and travels toward the major thrust side, it again hits the cylinder bore, causing vibration. The cylinder bore vibration can also be observed in Figure 6. The oscillatory motion of the piston repeats itself several times. Each time the piston hits the cylinder bore, it penetrates while maintaining its own peculiar motion. As the piston separates from the cylinder bore, the bore oscillates and continues to do so until the piston returns and strikes the cylinder bore again. It should also be mentioned that in both case study models, the cylinder pressure was obtained from Wave-Ricardo.[14] Typical cylinder pressures occurring at 1500 engine RPMs and 50 Manifold Absolute Pressure , for both motoring and firing engine conditions obtained from Wave-Ricardo and used in the case studies are given in Figure 7.

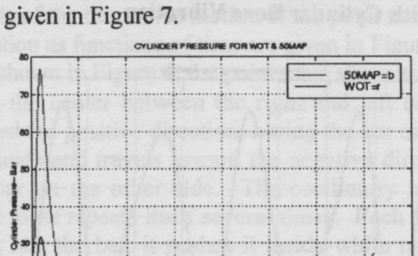

Figure 7: Cylinder Pressure For Wide Open Throttle & 50 Manifold Absolute Pressure @ 1000 RPM

In summary, piston kinematics and dynamics as well as the cylinder block vibration were discussed to better understand piston slap noise.

5. BLOCK VIBRATION

As previously mentioned, there are two approaches to study piston slap noise. The first approach involves studying the transverse motion, piston tilt and the piston impact forces. The second approach models these as well as cylinder block vibration.

The first approach is not complete because it does not provide a link between the analytical results to compare to experimental results. This is because the analytical results provide only the piston motion while the experimental results only measure the block vibration. Therefore, there can be correlation between the analytical work and the experimental data. To resolve this, measurements of the piston motion can be directly obtained. Although it is very tedious and expensive, the Grasshopper linkage[15] can measure the piston motion, yet still does not provide the block vibration. A grasshopper linkage is a device that measures the distance of the piston in motion in respect to the cylinder bore.

To utilize the efforts of the first approach, a link must be provided between the piston impact forces and block vibration. A study was performed to transform the piston impact forces to the forces represented along the major and minor thrust sides of the cylinder bore. The upper and lower major thrust and minor anti-thrust impact forces are obtained from either the code developed in Section 4 or any other commercial program as long as these four forces are provided. A linear distribution function was used to divide the piston impact force as a given time or crank degree on the nodes along the major or minor side. In this study, there were 16 nodes on the major thrust side and 16 nodes on the minor anti-thrust side for each cylinder bore which were unevenly distributed. Equation (5-1) describes the conversion of the piston impact force at a given time along the major and minor thrust sides. This equation represents the balance of the forces and moments at a given node as shown in Figure 8.

$$F_{node-i} + F_{node-j} = F_{impact-force}$$

$$-F_{node-j}(d_1 + d_2) + F_{impact-force} d_1 = 0 \qquad (5\text{-}1)$$

where d_1 and d_2 are the location of node-i and node-j with respect to where the piston impact force strikes the cylinder bore. Upon the completion of the engine cycles that result in a rotation of 720°, there are 32 time traces describing the forces that have impacted the cylinder bore. Since these 32 traces are in the time domain, a program was developed to transform them to frequency domain and generate the case control required to run the frequency response analysis of the engine block due to these forces. These forces were phased according to the firing orders for the V8 engine and then applied to the proper cylinders. A few of the force traces applied are shown in Figure 9. NASTRAN Modal Frequency Response Solution was performed on the input deck to provide the frequency response of the engine block. After the results were obtained from NASTRAN, they were reformatted from frequency domain into time domain. The engine block vibration results were translated into Hypermesh[16] format using Hmnast. This format allowed the vibration of the engine block to be viewed visually. At this stage, the vibration traces corresponding to any node of the engine block can be compared with the block vibration information obtained by accelerometers in an experimental test setup. This process can help not only in the validation of the engine block vibration due to piston slap but can also offer a good understanding between the piston impact forces and the engine block vibration. It should be mentioned that this methodology is the uncoupled approach for obtaining the block vibration information due to piston slap forces as compared to the direct approach of obtaining the block vibration. To demonstrate the feasibility of the uncoupled approach, the required steps discussed previously were taken. The results of the engine block vibration are given in Figures 10 and 11

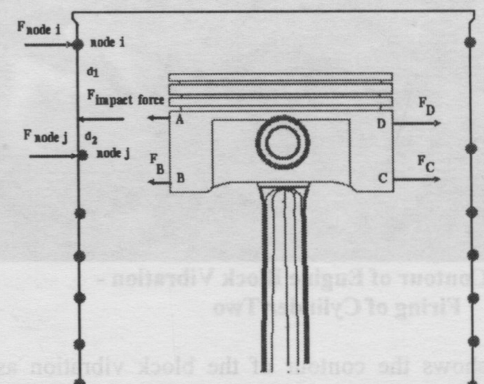

Figure 8: Impact Forces Mapped on the Cylinder Bore

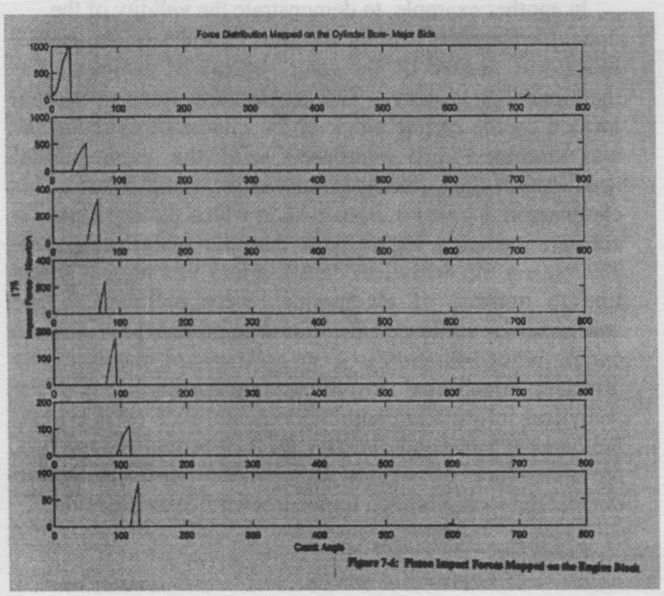

Figure 9: Force Traces on the Cylinder Bore

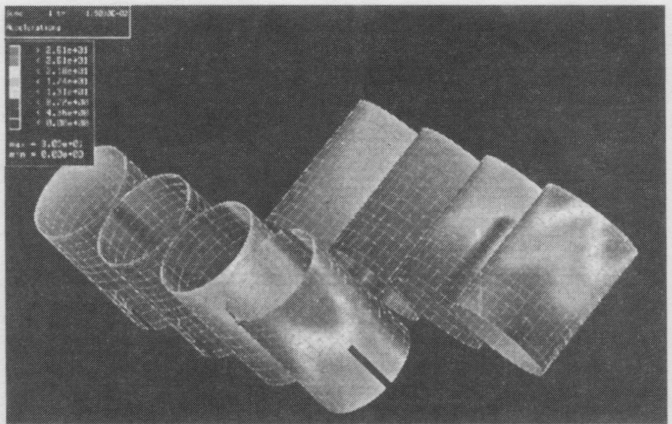

Figure 10: Contour of Engine Block Vibration -Firing of Cylinder One

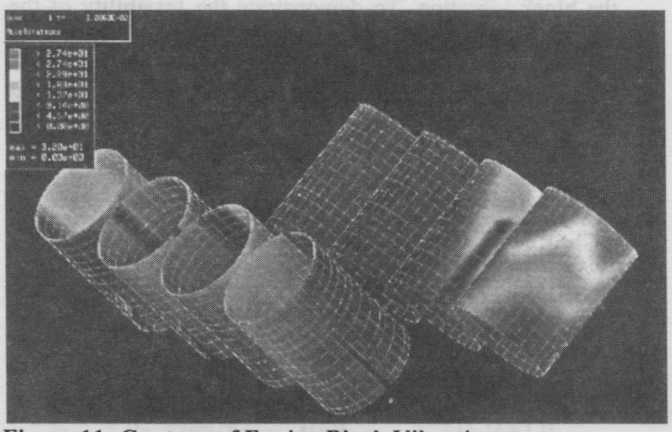

Figure 11: Contour of Engine Block Vibration - Firing of Cylinder Two

Figure 10 shows the contour of the block vibration as cylinder one fires while Figure 11 shows the contour of the block vibration as cylinder two fires. As shown in both figures, when the firing occurs, there is a higher block vibration intensity corresponding to that particular cylinder.

In another example, to demonstrate the validity of the uncoupled approach, only the first cylinder of the engine block was excited by the same sources of piston slap as mentioned previously. The acceleration trace of a point located on the engine block in the middle of cylinder one was obtained and compared with the experimental acceleration data corresponding to the same point. This comparison is given in Figure 12 in which the experimental acceleration has a higher peak than the analytical results. The reason the analytical data has less vibration is that a limited number of eigenvalues were included in the analysis. In summary, the direct approach provides the engine block vibration in a straightforward manner. The direct approach also simplifies comparisons between the analytical information and experimental data by providing the block information directly. In the uncoupled approach, the same block vibration is still obtained, yet the method to obtain the block vibration requires several extra steps.

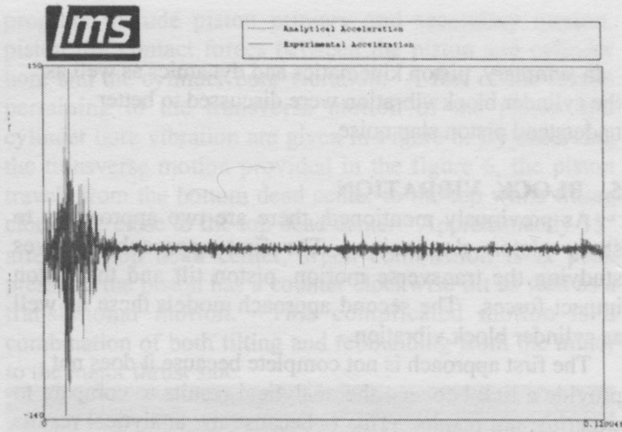

Figure 12: Analytical/Experimental Comparison of a Point Located on the Engine Block Corresponding to Cylinder One

6. CONCLUSIONS

A computer model was developed to understand the phenomenon of piston slap in conjunction with block vibration. Along with the analytical work, a series of experimental tests was conducted. The correlation between the analytical and experimental results was satisfactory. The analytical tools developed in this study predicted the occurrence of the piston slap through a comparison with the experimental work. To verify and extend the analytical work discussed here, a series of experimental parametric studies of the Grasshopper technology were implemented and will be discussed in detail in a subsequent paper

ACKNOWLEDGMENTS

The authors would like to thank General Motors Corporation for their full support and commitment to this study.

REFERENCES

1. C. Caccavaqri. 1971 Noise and Vibration Control Engineering Proceedings of the Purdue Noise Control Conference, Purdue University, Lafayette, Indiana.

2. Sander W., Steidle W. and Wacker E. Piston Movement and its Influence on Noise of Automotive Engines, Society of Automotive Engineers, Inc., Detroit, Michigan 1979.

3. DeJong, Richard. Vibrational Energy Transfer in a Diesel Engine, diss., Massachusetts Institute of Technology, 1976.

4. The outcome of the conference resulted in the publication of Diesel Engine Noise, 1980.

5. Ohta, Kazukide; Irie, Yoshihiko; Yamamoto, Kiichi and Ishikawa, Hideyuki. Piston Slap Induced Noise and Vibration on Internal Combustion Engines--1st Report Theoretical Analysis and Simulation.

Society of Automotive Engineers, Inc., Detroit, Michigan 1987.

6.Kamp, Harmut and Spermann, Johannes. New Methods of Evaluating and Improving Piston Related Noise and Internal Combustion Engines, Society of Automotive Engineers Inc., 1995.

7. Nakada, Teruo; Yamamoto, Atsushi and Abe, Takeshi. A Numerical Approach for Piston Secondary Motion Analysis and its Application to the Piston Related Noise, Society of Automotive Engineers, Inc. 1997.

8. MATLAB is a high-performance Numeric computation and Visualization Software developed by The Math Works, Inc. that integrates numerical analysis, matrix computation, signal processing and graphics.

9. Meirovitch, Leonard. Elements of Vibration Analysis. McGraw-Hill, Inc. New York, 1986.

10. Refer to Reference 5.

11. NASTRAN is an finite element code developed and maintained by the MacNeal-Schwendler Corporation.

12. The LMS CADA-X module developed by LMS International Corporation. For more information, refer to LMS CADA-X. System Solutions for Acoustics, Structural Dynamics and Durability, LMS International.

13. Borse, G.J., Numerical methods with MATLAB. PWS Publishing Company, Boston, 1997.

14. Wave-Ricardo is a commercial computer simulation code used to model a complete internal combustion engine. The basic engine model consists of a multi-cylinder thermodynamic cycle simulation that provides several engine types.

15. Siavoshani, Saeed J. Analytical and Experimental Study of Piston Slap in Conjunciton with Block Vibration. diss., Oakland University, 1998.

16. Hypermesh is a commercial code used as a pre-processor and post-processor for preparing finite element mesh and viewing the results.